NANOMATERIALS
SCIENCE & ENGINEERING
Vol. 2, No. 4, pp. 175-182 (2020)

RESEARCH ARTICLE

https://doi.org/10.34624/nmse.v2i4.21072

Carbon fibber reinforced polymer use in space launch vehicle propellant tanks - concept and finite element method study

Miguel Fernandes* and Francisco Brojo

Aerospace Sciences Department, University of Beira Interior. Convento de Sto. António. 6201-001 Covilhã. Portugal
**Corresponding author, e-mail address: mig_16_ang@hotmail.com*

Received 10 June 2020; accepted 10 December 2020; published online 15 December 2020

ABSTRACT

Weight reduction is a never-ending goal in aerospace engineering, especially for a space launch vehicle (SLV), were every gram of mass has a penalty in the vehicle's performance. Since propellant tanks generally weigh more than half of the dry mass of a SLV, it is particularly advantageous to implement composite materials in their construction. Yet, difficulties with oxygen compatibility, permeability and manufacturing maturity dictate that aluminium alloys with high lithium content are still the state of the art in this field. Recent developments in the aerospace composites industry are starting to change this perception, especially regarding Carbon Fibber Reinforced Polymer (CFRP) application. Hence this study, which aims to propose an integral CFRP propellant tank concept and determine mass savings by comparing it to a metallic baseline, through finite element method (FEM) analysis with simulated flight loads. Tank dimensions, geometry and loads were chosen for micro-satellite SLV application. Also, Altair's Optistruct solver was used for FEM calculations, with Altair's HyperWorks for pre and post-processing. A mass reduction of close to 35% has been obtained with comparison to the metallic baseline design for the same boundary conditions. Therefore, a sound and competitive design for a micro-satellite SLV propellant tank has been successfully achieved.

1. INTRODUCTION

Propellant tanks account for more than half of the dry mass and close to 90% of the volume of a space launch vehicle (SLV) [1, 2]. This makes mass reduction in propellant tanks to have a major potential effect in the SLV's performance, as they are a centrepiece in its design. Composite materials, particularly carbon fibber reinforced polymers (CFRP), exhibit superior specific-strength and specific-stiffness than the currently used metallic alloys, even though they are possibly 30 to 40% lighter [3].

Propellant tanks are mostly cylindrically shaped to better use the space inside a missile-like vehicle, whilst holding the propellants under pressure. In vertical launch vehicles, they usually double as the main structure, becoming “load-bearing” or “integral” propellant tanks [1, 2]. Moreover, because of the long cylindrical shapes, stiffness is as important as strength, to avoid buckling. Hence, they are expected to endure mostly axial compression and hoop stresses.

However, some of the properties of composite materials present challenges for their application in propellant tanks. First, there is always some rate of propellant diffusion with cryogenic propellants due to matrix porosity, but laminates that avoid micro-cracking and internal manufacturing imperfections have achieved acceptable diffusion rates [3]. Leakage can occur through the porosity of the matrix, damage by delamination and accumulation of micro-cracks between the matrix and fibres [3]. Micro-cracks can be caused by the different thermal expansion coefficients of the materials during thermal cycles or by lighter impact damage. In addition, the chemical compatibility with oxygen is an issue, as organic materials can ignite in strong oxidising environments under certain conditions. Even though CFRPs often fail some of the standard flammability tests, work is being done to create modified flammability acceptance tests for propellant tank application [3, 4].

Several works have been conducted on the chemical stability of epoxies in pure oxygen environments [5, 6]. CFRPs typically have cryogenic strength performance close to room temperature [7]. Their upper service temperatures, slightly above 100 degrees Celsius [8], are sufficient for launch vehicle application as they are now commonly used in solid propellant motor structural fuselages [2], with special care for thermal insulation.

The aim of this work is to develop an integral CFRP propellant tank concept and determine mass savings by comparing it to a metallic baseline, through finite element method (FEM) analysis with simulated flight loads.

2. LAUNCH VEHICLE AND TANK CONCEPTS

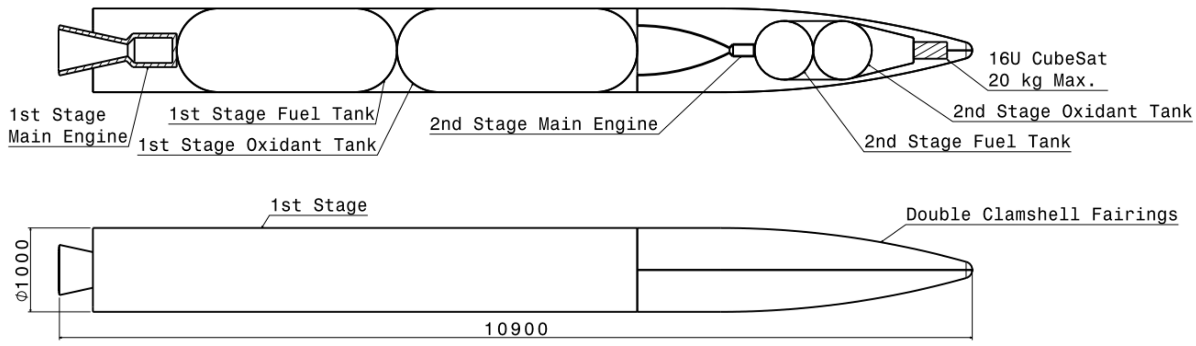

Figure 1. SLV Concept (section and exterior views; dimensions in millimetres).

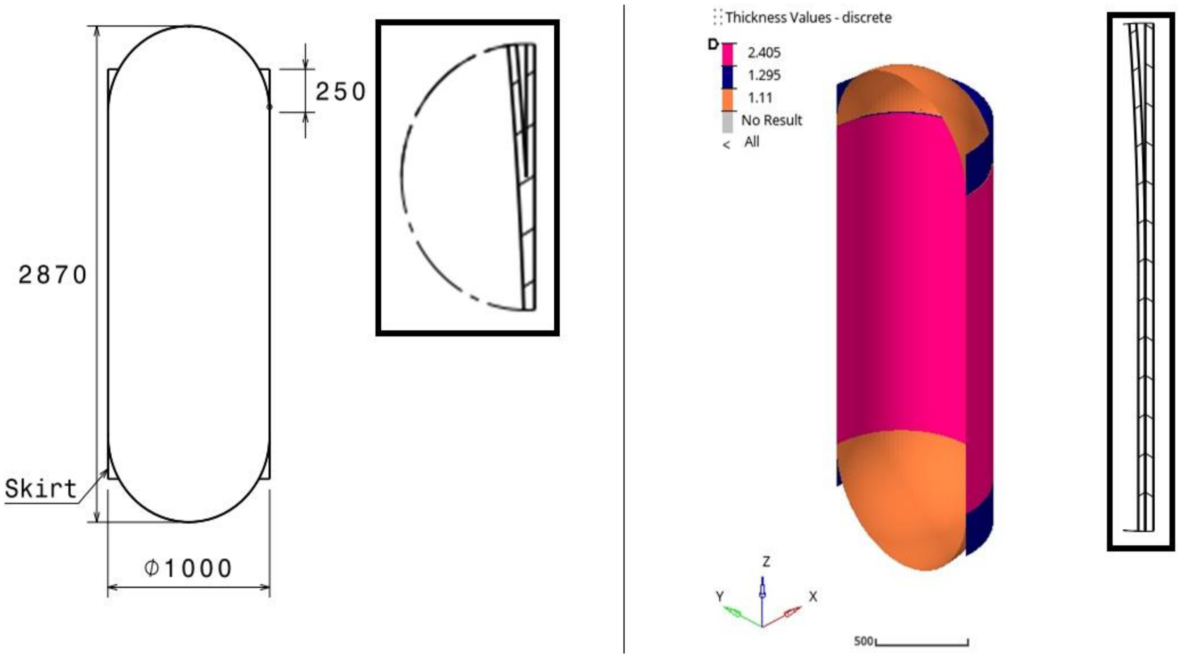

Figure 2. Aluminium (left) and composite (right) tank concepts with the respective skirt joint details.

The geometric and performance data of a space launch vehicle is required to calculate the fight loads to which the propellant tank will be subjected, wherefore a small SLV conceptual design was developed. Then, a metallic tank concept was designed for baseline comparison, followed by an equivalent CFRP propellant tank design. With the tank geometry defined, the respective FEM models were created and simulated to assess static strength and static stability behaviour taking into account safety factors used in launch vehicle design, as per Anon. (2016) [9].

Figure 1 shows the concept of the launch vehicle. As today's electronics allow for the construction of utilitarian microsatellites (10 to 100 kg) and nanosatellites (1 to 10 kg), this concept was designed for the dedicated launch of small payloads of up to 20 kg to orbit. It is a 3,000 kg gross weight, two-stage, expendable SLV with composite construction and cryogenic propellants for their superior efficiency. The upper tank of the first stage is the one being analysed in this work.

The aluminium propellant tank baseline design is shown in Figure 2 (left side). Fabrication is assumed to be through forming and welding with a thickness of 1 mm. It is an integral tank, with the interface skirts to connecting to the rest of the vehicle, and spherical domes. The detail (Figure 2, left side) shows the transition zone between the tank itself and the skirts. Table 1 gives the chosen aluminium alloy mechanical properties. For the composite tank (Figure 2, right side), the overall

Table 1. Aluminium properties.

AL 2219-T87				
Tensile Yield Strength [MPa]	Tensile Ultimate Strength [MPa]	Density [kg.m^-3]	Poisson's Ratio -	Elastic Modulus [MPa]
352	434	2,851	0.33	72,395

Table 2. CFRP properties.

AS4 Carbon Fiber Tow/Toughened Epoxy						
E1 [MPa]	E2 [MPa]	NU12 -	G12 [MPa]	G1Z [MPa]	G2Z [MPa]	Density [kg.m^-3]
141,000	9,750	0.267	5,200	5,200	3,190	1,580
Xt [MPa]	Xc [MPa]	Yt [MPa]	Yc [MPa]	S [MPa]	ILSS [MPa]	Thickness [mm]
2,200	1,500	81	260	80	128	0.185
E1 - Longitudinal Elastic Modulus E2 - Transverse Elastic Modulus NU12 - In-Plane Major Poisson Ratio G12 - Longitudinal In-Plane Shear Modulus G1Z - Longitudinal Out-of-Plane Shear Modulus G2Z - Transverse Shear Modulus Xt - Longitudinal Tension Strength Xc - Longitudinal Compression Strength Yt - Transverse Tension Strength Yc - Transverse Compression Strength S - In-Plane Shear Strength ILSS - Interlaminar Shear Strength						

dimensions are the same. No sandwich construction is used to avoid delamination caused by trapped gases due to permeation. Table 2 provides the mechanical properties of the selected carbon fibber tows with toughened epoxy matrix. The composite tank assumes filament wound manufacturing of an internal tank and external barrel. Both sub-components are then co-cured to form a single part. A detail of the transition zone can be seen in Figure 2, right side.

These are the ply orientations for both sub-components:

- [+30/+60/-30/90/+30/-60/-30] for the external barrel.
- [-45/+45]$_3$ for the internal tank.

3. FEM MODEL

After modelling the tank geometry, a FEM model of each tank was made. Bi-dimensional quadrilateral shell elements of the 1st order were used with an element size of 25 mm. Regarding the element size, a convergence study was made with element sizes of 20 mm and 15 mm, and the maximum von Mises stress varied about 0.3%, therefore, the 25 mm element size was maintained.

A one-dimensional rigid multi-point constraint (MPC) element is attached to the upper skirt edge and its function is to evenly distribute the flight resultant forces and moments, as can be seen in Figure 3.

As for boundary conditions, the lower skirt edge nodes have their displacement constrained in all 6 degrees-of-freedom (6DOF) with single point constraints (SPC).

Concerning the software used, the solver package was Altair's Optistruct, with Hyperworks for pre- and post-processing. The FEM models were subjected to linear static and static instability analysis to compare the tanks strength and rigidity when subjected to the flight loads. For the linear static analysis, Optistruct employs the BCS solver that is based on the stiffness matrix method. The von Mises distortion energy criterion was used to access the strength of the ductile isotropic metallic tank, while for the CFRP tank, with orthotropic laminates, the Hoffman Failure Index (FI) quadratic criterion was used, assuming First Ply Failure (FPF).

As to the static instability analysis, an Optistruct linear buckling solver was used that makes a real eingenvalue extraction using the Lanczos method.

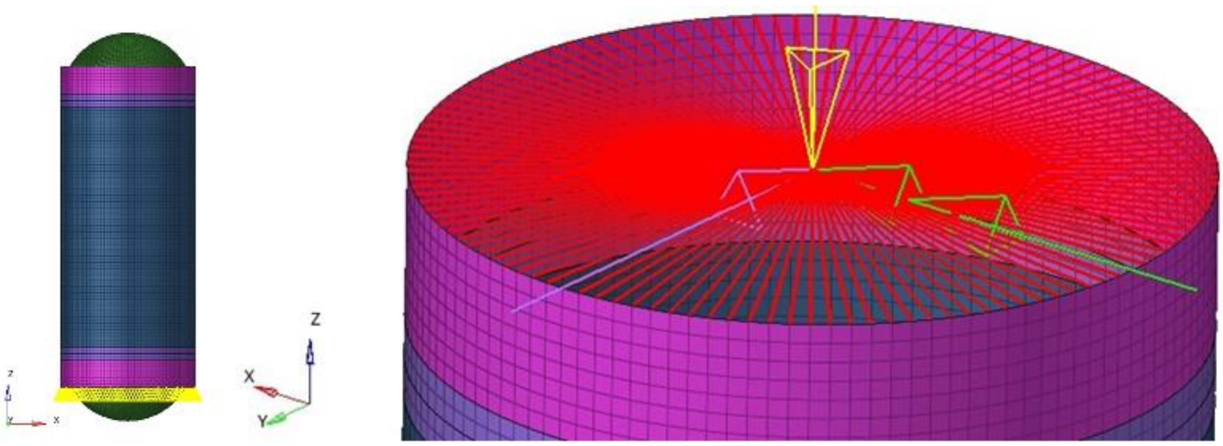

Figure 3. Propellant tank FEM model (left) and load application detail (right).

Table 3. Maximum tank loads.

Fz [N]	Fy [N]	Mx [N.m]	MEOP [MPa]	MSP [MPa]
8,831	3,083	11,338	0.578	0.13

Table 4. Load case definition.

LC	Load Case Name	Axial	Shear	Moment	Inertial [g]	Internal Press.
1	MEOP Proof	-	-	-	1.0	MEOP
2	Max. Compression	-Fz	-Fy	Mx	3.0	MSP
3	Max. Tension	-Fz	-Fy	Mx	3.0	MEOP
4	Pressure failure	-Fz	-Fy	Mx	3.0	0

Table 5. Factors of Safety (FoS) by load case.

LC	Load Case Name	FoS Metallic		FoS Composite		Buckling Knockdown Factor (K)
		Yield	Ultimate	Continuous	Discontinuous	
1	MEOP Proof	1.05	-	1.05	N/A	0.65
2	Max. Compression	1.25*	1.4*	1.5*	2.0*	
3	Max. Tension	1.25	1.4	1.5	2.0	
4	Pressure failure	-	1.0	1.0	N/A	

Assuming no imperfections, the first positive eigenvalue provides the factor of the load at which the structure will buckle for the respective load case.

Table 3 contains the maximum resultant flight loads and internal pressures that were calculated for the launch vehicle shown previously. MEOP is the maximum expected operational pressure, including the hydrostatic pressure contribution of the contained propellant, while MSP is the defined minimum stabilizing pressure. Fz, Fy and Mx are the resultant maximum compression and shear forces and bending moment, respectively, and surmise all flight loads acting on the vehicle.

Table 4 has the load case definition, while Table 5 shows the safety factors (from Anon. (2016) [9]) included in the respective load cases. The first load case is to access the behaviour of the tank under maximum pressure and has no flight loads applied. The second load case accounts for the tank operating near the minimum pressure (close to depletion), where the maximum compressive stresses might appear. The pressure for this load case has no factor of safety to prevent increasing the stabilizing effect that the internal pressure has on the structure, and that may increase rigidity. This is noted as an asterisk in the load case safety factors. On the other hand, the third load case has all loads at full strength with the appropriate factors of safety. Finally, the fourth load case has no internal pressure or factors of safety. This load case is to access the structural behaviour in case of a sudden critical pressure drop during the flight, like in the event of a rupture or valve malfunction. Regarding the factors of safety, they are different for metallic and composite materials. Metallic load cases also have separate factors for yield and ultimate tensions, and composite materials for zones with and without discontinuities. A buckling knockdown factor is applied to the eingevalue factors to account for material and geometric imperfections.

4. RESULTS

After design and modelling iterations, the final mass for the aluminium tank was 30.18 kg and 19.65 kg for the CFRP tank. So, by changing the material from aluminium to CFRP, mass savings of close to 35% were achieved in spite of the increased thickness of the composite laminates. The strength and rigidity analysis results are surmised by Table 6 for the aluminium tank and Table 7 for the CFRP tank. It can be observed that

Table 6. Aluminium tank results.

Aluminium Tank					
LC	von Myses [MPa]	MoS -	Max. Disp. [mm]	Buckling Factor -	MoS (w/ K-factor) -
1	240.37	0.46	1.96	N/A	N/A
2(y)	108.14	2.26	2.60	2.93	0.90
3(y)	333.20	0.06	4.05	2.62	0.70
4	46.63	8.31	2.03	3.65	1.37
2(u)	114.32	2.80	2.90	N/A	N/A
3(u)	373.18	0.16	4.54	N/A	N/A

Table 7. CFRP tank results.

CFRP Tank				
LC	Hoffman FI -	Max. Disp. [mm]	Buckling Factor -	MoS (w/ K-factor) -
1	0.18	1.25	N/A	N/A
2	0.09	2.84	2.65	0.72
3	0.37	4.24	2.46	0.60
4	0.03	1.84	3.99	1.59
2(disc)	0.12	3.75	N/A	N/A
3(disc)	0.55	5.65	N/A	N/A

load case 3 is the critical one, having the highest stresses and the lowest bucking margin of safety.

The two bottom rows show the results with the greater factors of safety for the ultimate strength (aluminium, Table 6) and discontinuous zones (CFRP, Table 7).

In Figure 4 the two left side images (a and b) show the criterion results for both tanks for the third load case (LC03) with the greatest factors of safety. It can be seen that the aluminium tank is stressed close to the ultimate strength of the material (a) as this is the most critical load case. In the composite tank, only the zones with discontinuities are relevant for this factor of safety, and, therefore, are the only ones shown (b). This was the limit that led to a final increase in the composite interior tank thickness during the design process, hence, the final composite design is lightly loaded.

The two right side images (c and d) show the criterion results for the fourth load case (LC04) for both tanks, were the internal relative pressure is zero. The bending and shear effects are clearly visible with one side of the tanks being more loaded. By comparing both load cases, it is noticeable that the internal pressure is the most critical load, as the other load cases have a similar stress distribution to LC03.

Lastly, Figure 5, to the left (a and b), shows LC03 criterion distribution, with the lower factors of safety for yield and continuous zones, while to the right (c and d) are the buckling failure modes for the same load case with the respective margins of

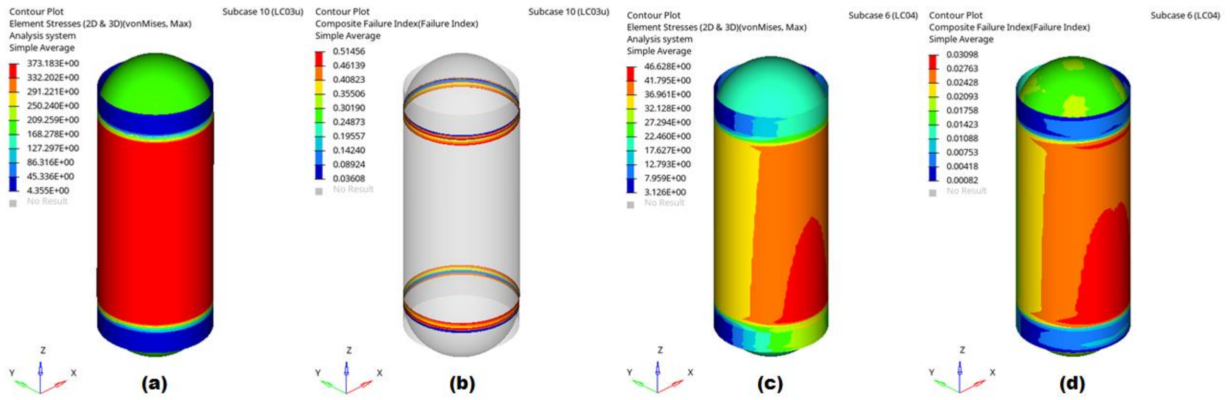

Figure 4. Results: (a) LC03 - Aluminium, von Mises Ultimate; (b) LC03 - Discontinuous CFRP, FI; (c) LC04 - Aluminium, von Mises; (d) LC04 - CFRP, FI.

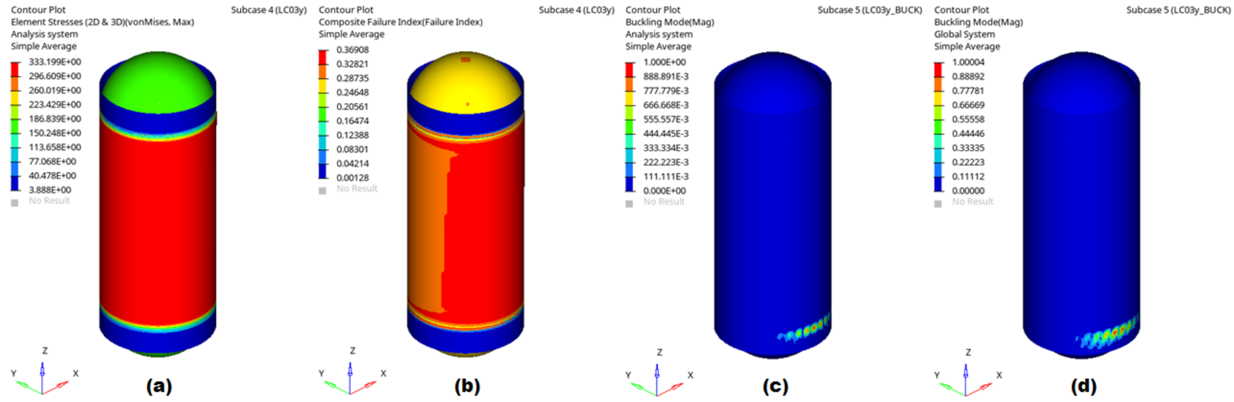

Figure 5. Results: (a) LC03 - Aluminium, von Mises Yield; (b) LC03 - Continuous CFRP, FI; (c) LC03 - Aluminium, Buckling, MoS 0.7; (d) LC03 - CFRP, Buckling, MoS 0.6.

safety. Buckling behaviour is similar in the other load cases and therefore not shown.

No positive eigenvalues could be found for the first load case. This should be due to the stabilizing effect of the internal pressure and no other significant loads being applied to the tank.

As it was previously noted, the composite tank concept is lightly loaded and sub-optimized owing to discreet ply increase as a function of fibber roving thickness. For the internal tank subpart, the ply number increase was done to decrease in-plane shear stress concentrations at the discontinuous zones in the worst load case. As to the external barrel subpart, the increase of plies was done to increase rigidity of the composite tank at the skirts for bulking knockdown factor compliance. Also, the internal tank ply orientation is optimized for the spherical domes.

4. CONCLUSION

As can be seen, an equivalent CFRP composite propellant tank design has been achieved with 35% mass reduction. However, the final thickness of the composite tank is greater than its aluminium counterpart, even though no sandwich construction was used.

Also, this concept has potential for further mass reduction. For example, stiffeners can be applied to the barrel to increase rigidity and allow ply reduction.

We believe that small launch vehicles can benefit the most from composite components. This is because of the trend of the mass ratio of a launch vehicle becoming worse with the decrease in launch vehicle gross mass, leading to less structural efficiency in small launch vehicles.

ACKNOWLEDGEMENTS

The current study was funded in part by Fundação para a Ciência e Tecnologia (FCT), under project UID/EMS/00151/2013 C-MAST, with reference POCI-01-0145-FEDER-007718. Also, the authors would like to thank Altair for providing the HyperWorks FEM software package that made this study possible.

REFERENCES

[1] D. H. Huang and D. K. Huzel, Modern Engineering for Design of Liquid-Propellant Rocket Engines, American Institute of Aeronautics and Astronautics, Washington DC (1992).
[2] G. P. Sutton and O. Biblarz, Rocket Propulsion Elements, 9th ed., John Wiley & Sons, Inc., Hoboken, New Jersey (2016).
[3] R. J. Wright, D. C. Achary, and M. C. Mcbain, in Composite Development & Applications for RLV Tankage, AIAA/ICAS International Air and Space Symposium and Exposition, Dayton, OH (2003).
[4] D. A. McCarville et al., *Compr. Comp. Mat.* II, **3**, 153 (2018).
[5] G. Wang et al., *Mater. Sci. Eng. B Solid-State Mater. Adv. Technol.*, **132(1-2)**, 70–73 (2006).
[6] T. Sun et al., *High Perform. Polym.*, **26(3)**, 319–325 (2014).
[7] R. P. Reed and M. Golda, *Cryogenics (Guildf).*, **34(11)**, 909–928 (1994).
[8] D. Cree et al., *J. Compos. Constr.*, **19(2)**, 04014043 (2015).
[9] Anon., NASA-STD-5001B W/ CHANGE 1 - Structural Design and Test Factors of Safety for Spaceflight Hardware, Washington DC (2016).